Seismic imaging of oil production rate

Valeri A. Korneev, Dmitry Silin, Lawrence Berkeley National Laboratory, Berkeley, California
Gennady M. Goloshubin, University of Houston, Texas,
Viacheslav Vingalov, ZapSibNIIGG, Tyumen,Russia

Abstract

Field and laboratory data indicate anomalously high reflectivity from fluid-saturated reservoirs at the low-frequency seismic range. It also has been observed that the reflected signal is frequency-dependent and is strongly related to the reservoir flow properties. We have obtained an asymptotic representation of the seismic reflection from a fluid-saturated porous medium in the low-frequency domain. The frequency-dependent component of the reflection coefficient is proportional to the square root of the product of frequency of the signal and the mobility of the fluid in the reservoir. This provides an opportunity for locating the most productive zones of the field before drilling. In the presented example we quantify low-frequency imaging amplitude attribute in terms of reservoir fluid mobility and reservoir production rate.

Theory

We consider reflection of a plane elastic compression wave of an angular frequency ω from the boundary between dry and fluid-saturated elastic porous media. Within a reasonable range of rock and fluid properties, the dimensionless parameter $\varepsilon = \frac{\kappa \varrho_b}{\eta}\omega$ is small at low (below 1 kHz) seismic frequencies. Here κ is the reservoir rock permeability, η is the viscosity of the reservoir fluid and ϱ_b is the bulk density of the reservoir fluid-rock system. In (Silin *et. al.*, 2004), we have obtained an asymptotic expression of the reflection coefficient R in the following form:

$$R = R_0 + R_1 (1+i)\sqrt{\frac{\kappa \varrho_b}{\eta}\omega} \qquad (1)$$

Here the coefficients R_0 and R_1 are dimensionless functions of the mechanical properties of the fluid and rock, which include the porosity, the densities, and the elastic coefficients. At $\varepsilon = 0$ the absolute value of the reflection coefficient attains its low-frequency maximum. Equation (1) has been obtained from basic principles of filtration theory and elasticity. In particular, the derivation includes a dynamic version of Darcy's law with a relaxation time τ. The latter is in linear relation with the tortuosity factor. If the relaxation time is large, *i.e.,* $\tau > 1/\omega$, then the asymptotic relationship (1) must be replaced with

$$R = R_0 + \tilde{R}_1\sqrt{i - \tau\omega}\sqrt{\frac{\kappa \varrho_b}{\eta}\omega} \qquad (2)$$

The explicit formulae for the coefficients are given in (Silin *et. al.*, 2004).

We define an imaging attribute $A(x, y)$ as being proportional to the first derivative with respect to the frequency of the reflected amplitude. Here x and y are lateral coordinates of the reservoir. From (1),

$$A(x,y) \approx C\,(\kappa/\eta)^{1/2} \qquad (3)$$

where the coefficient C is a complex function of frequency, and of the mechanical properties of the fluid and the skeleton. At a given signal frequency, the coefficient C can be estimated using well data. Assuming that the production rate at a well is proportional to the fluid mobility in the nearby formation and that only the rock permeability is a function of the coordinates, we can fit the data with a theoretical curve linking the production rate and the imaging attribute.

Application

We have analyzed seismic data from a 3 km-deep Jurassic sandstone reservoir. The map of the target horizon J1 is shown in Figure 1. The reservoir thickness is approximately 8-10 m and the mean porosity is about 17-18%. From the 15 operating wells, 7 produced oil and 6 produced water. The other two wells produced and an approximately equal mixture of oil and water. Four wells, whose data were used for calibration, are shown in Fig. 2. From these four wells, three (76, 91, 95) produce oil whereas the fourth one (9) produces mostly water. The data from the other 11 wells were used for *a posteriori* verification of the mapping only. Fig. 1 shows a time map of the target horizon J1.

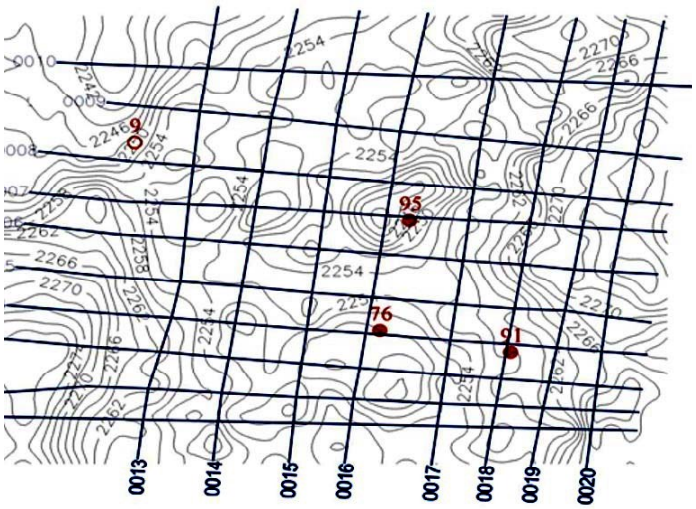

Fig. 1 Structural time map of the reservoir surface with location of 4 calibration wells, three of which (76, 91, 95) produce oil whereas the fourth one (9) produces water. Note a poor correlation between medium structure and fluid.

Fig. 2 shows the results of frequency-dependent processing of this dataset. The seismic imaging map includes the variation of the amplitude of the target reflected wave at a low frequency (12 Hz) relative to the amplitude of the same wave at a high frequency (40 Hz). The imaging results *predicted* the location of oil-water contact. These results were confirmed by the

well data. All wells producing water are outside of the oil-saturated region. The wells with the highest oil production rate (*e.g.*, wells 91 and 86) are found close to the zones of the high deviation of the map attribute at low frequencies.

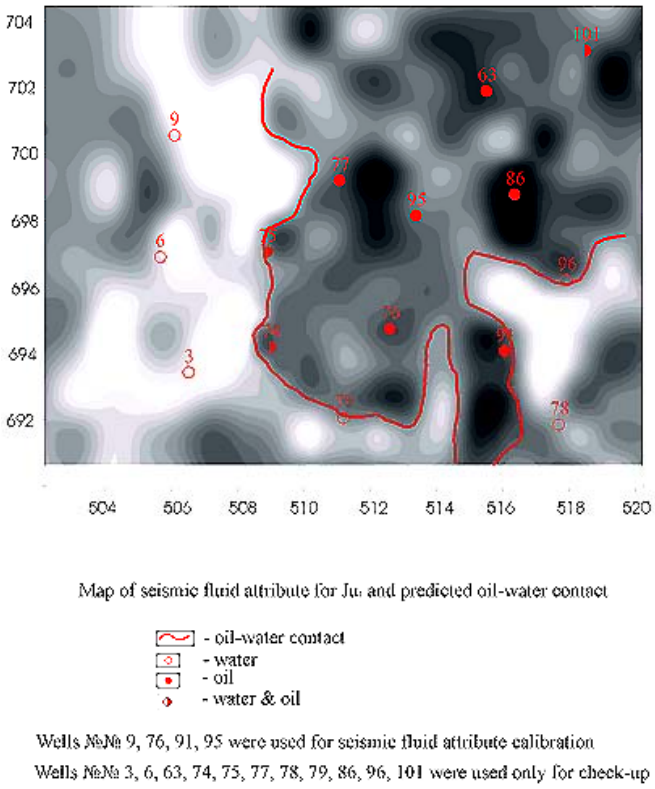

Fig. 2 A blind test of the ability of frequency-dependent processing and interpretation to map the oil-water contact using the low-frequency part of seismic data. The seismic and well data recorded in Central Siberia. The seismic image shows the difference of low-frequency reflectivity at 12 Hz to the one at 40 Hz centered frequency, the predicted oil-water contact, and the locations of the calibration wells and the wells used for testing purposes. (Goloshubin, *et al*., 2002)

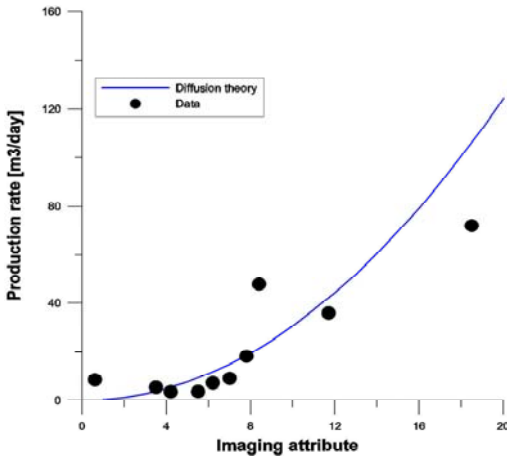

Fig. 3 The oil production rate vs. the imaging attribute. Data taken from oil field shown on Fig. 4. The theoretical blue line is computed using the low-frequency asymptotic solution (12).

The data has been processed using the imaging attribute (3). Figure 3 shows the measured production rates for the oil field from Fig. 2, and the theoretical curve, which was calibrated using just one well data point. Using this fit, we convert the attribute map from Fig. 2 into a production rate map. The result is shown in Figure 4.

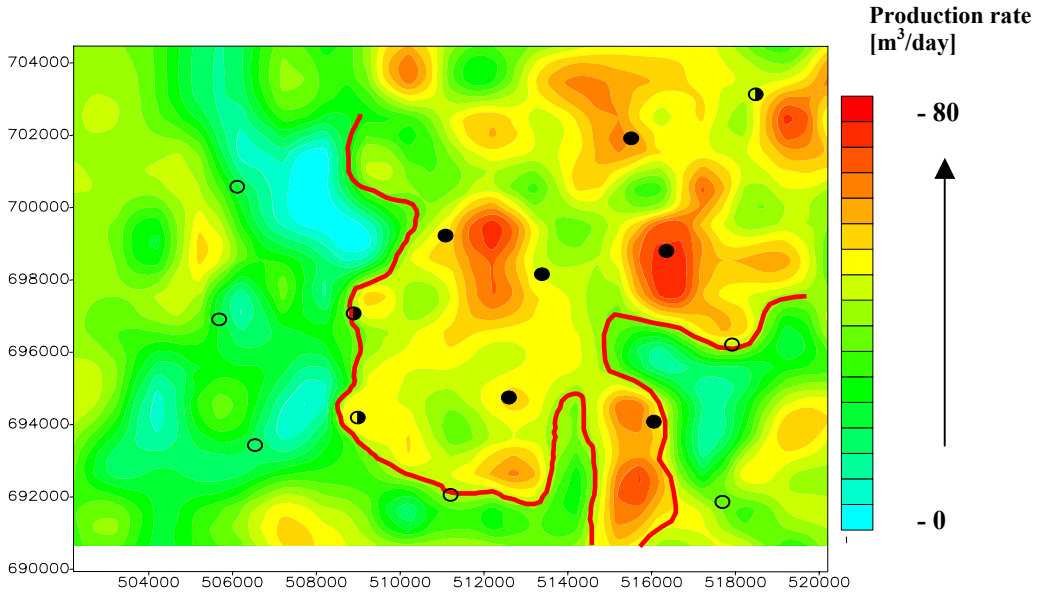

Fig. 4. Map of the production rate.

Conclusions

The application of low-frequency analysis and derived asymptotic allowed us to map the potential reservoir productivity. This method can be used for detecting and monitoring liquid saturated areas in porous and fractured reservoirs.

Acknowledgments

This work is a result of collaboration of Center for Computational Seismology at Ernest Orlando Lawrence Berkeley National Laboratory where it was supported by the Office of Science, Office of Basic Energy Sciences, Division of Engineering and Geosciences of the U.S. Department of Energy under Contract No.DE-AC03-76SF00098, and Western Siberian Research Institute of Geology & Geophysics (ZapSibNIIGG). Data are courtesy of Surgutneftegas. Authors are grateful to Fred Hilterman for his helpful comments.

References

Goloshubin, G.M., V.A.Korneev, V.A., and Vingalov, V.M., 2002, Seismic low-frequency effects from oil-saturated reservoir zones, SEG Meeting,: Salt Lake City.

Silin, D. B., Korneev, V. M., Goloshubin, V. M., and Patzek, T. W., 2004, A Hydrologic View on Biot's Theory of Poroelasticity. LBNL Report 54459